Pergamon

Journal of Structural Geology, Vol. 16, No. 6, pp. 853 to 865, 1994
Elsevier Science Ltd
Printed in Great Britain
0191–8141/94 $07.00+0.00

The transition from magmatic to high-temperature solid-state deformation: implications from the Mount Stuart batholith, Washington

ROBERT B. MILLER

Department of Geology, San Jose State University, San Jose, CA 95192-0102, U.S.A.

and

SCOTT R. PATERSON

Department of Geological Sciences, University of Southern California, Los Angeles, CA 90089, U.S.A.

(*Received* 28 *May* 1992; *accepted in revised form* 28 *July* 1993)

Abstract—Criteria for syntectonic emplacement of plutons are commonly ambiguous. The strongest single criterion is probably the preservation of a continuous transition from submagmatic to high-temperature solid-state deformation. This transition is not commonly documented. An exception is the Mount Stuart batholith, which displays a variety of syntectonic structures within its sheared northeastern margin, including the following: (1) *S–C* fabrics that range from submagmatic to high-temperature solid-state;(2) solid-state foliation and lineation defined by amphibolite-facies assemblages that overprint and are parallel to magmatic foliation and lineation; (3) folds of magmatic and solid-state foliation that have hinge lines parallel to magmatic and solid-state lineation and to equivalent structures in wall rocks; (4) dikes that were folded and boudinaged over a wide range of rheological states with boudin necks locally filled by tonalite; (5) pegmatite dikes and mineralized joints that are sub-perpendicular to magmatic and solid-state lineation; and (6) submagmatic and high-temperature solid-state ductile shear zones.

We suggest that many plutons emplaced during regional deformation do not preserve evidence for syntectonic deformation because of the transitory nature of the submagmatic state and the obscuring effects of post-emplacement deformation. Syntectonic features are most likely preserved in plutons cooled at slow to moderate rates, or in plutons deformed at high strain rates during emplacement. The optimum conditions for preservation may occur in plutons emplaced along fault zones in the mid-crust, such as the Mount Stuart batholith, and in intrusions at deeper levels that were rapidly exhumed and/or intruded during the waning stages of regional deformation.

INTRODUCTION

CRITERIA for the timing of pluton emplacement relative to regional deformation are commonly ambiguous (e.g. Paterson & Tobisch 1988). For example, in most theoretical models of granite emplacement many, if not most, plutons are syntectonic (e.g. Pitcher 1979, Hutton 1988, Karlstrom 1989), yet it is difficult to demonstrate unequivocally such timing for individual plutons. Paterson *et al.* (1989) noted that individual timing criteria are rarely unambiguous and emphasized the importance of multiple criteria. They contended that the strongest evidence of syntectonic emplacement includes the following: a transition between parallel or subparallel magmatic and high-temperature solid-state foliation; high-temperature solid-state foliation in plutons continuous with lower temperature regional foliations; evidence that melt migration is controlled by regional deformation; and syntectonic porphyroblasts in wall rocks related to heating by the pluton. Perhaps the strongest case is where a continuous, geologically short-lived transition from submagmatic (flow in a crystal dominated system, but with sufficient melt to permit crystal sliding and movement of melt) to high-temperature, solid-state deformation is documented, particularly when a later high-temperature deformational event can be ruled out.

The nature of the transition from the submagmatic to solid state has important implications for emplacement models, for cooling and strain rates within plutons and their wall rocks, and for timing of emplacement relative to regional deformation. Relatively few studies of plutons, however, have documented this transition (e.g. Gapais & Barbarin 1986, Hollister & Crawford 1986, Blumenfeld & Bouchez 1988, Vernon *et al.* 1989, Bouchez *et al.* 1992, Karlstrom *et al.* 1993), despite the common interpretation of syntectonic emplacement. In this paper, we describe a variety of well-developed submagmatic and high-temperature solid-state structures in the Mount Stuart batholith of the North Cascades, Washington, that we interpret to record a continuum in deformation during emplacement. We discuss the implications of the deformation of this intrusion for syntectonic emplacement in general and speculate on why structures recording the transition from magmatic to submagmatic to high-temperature, solid-state deformation are not more commonly preserved in plutons.

GENERAL SETTING AND *P–T* CONDITIONS OF THE MOUNT STUART BATHOLITH AND ITS WALL ROCKS

The Mount Stuart batholith lies at the southern end of the crystalline core of the North Cascades, which is the southeast extension of the >1500 km long Coast Plutonic Complex (Fig. 1). It intrudes the pelitic Chiwaukum Schist on its northern and eastern margins and the ophiolitic, Upper Jurassic Ingalls Complex on its southeastern, southern and western margins (Fig. 2). The Ingalls Complex was thrust over the Chiwaukum Schist along the Windy Pass thrust (Miller 1985, 1988). Thrusting occurred at least in part after ~95 Ma, the inferred crystallization age (U–Pb zircon) (W. J. Hoppe in Miller 1985, S. A. Bowring written communication 1993) of the tonalite protolith of an orthogneiss that has been imbricated with the ophiolite. Imbricate slices in the upper plate are truncated by a 93 Ma phase of the batholith, and final movement on the Windy Pass thrust may have ceased during crystallization of the batholith (Miller & Paterson 1992) as discussed below.

Two nearly connected bodies comprise most of the Mount Stuart batholith, the southwestern body and the larger, more complexly shaped main body (Fig. 2). The batholith ranges in composition from gabbro to two-mica granodiorite, but is composed primarily of biotite–hornblende tonalite and lesser granodiorite (Pongsapich 1974, Erikson 1977, Anderson 1992). Tonalite and diorite from two localities in the main body yielded U–Pb zircon ages of 93.5 ± 0.5 Ma (Walker & Brown 1991) and 93.2 Ma ± 0.5 Ma (S. A. Bowring written communication 1990) that are inferred to date crystallization. A small mafic phase is slightly older at ~96 Ma (U–Pb zircon; Tabor *et al.* 1987). Some quantitative limits can be placed on the physical conditions during emplacement of the batholith. Anderson's (1992, personal communication 1992) thermobarometric analyses indicate that solidus temperatures range from >940°C for more mafic rocks to 642°C for granodiorites. The solidus for the tonalites ranges from 733 to 642°C, with liquidus temperatures in excess of 780°C (J. L. Anderson personal communication 1992). Application of the aluminium-in-hornblende and garnet–plagioclase–biotite–muscovite barometers indicates that pressures during crystallization were between ~ 1.7 and 3.7 kbar (6–13 km depth) (Anderson & Paterson 1991).

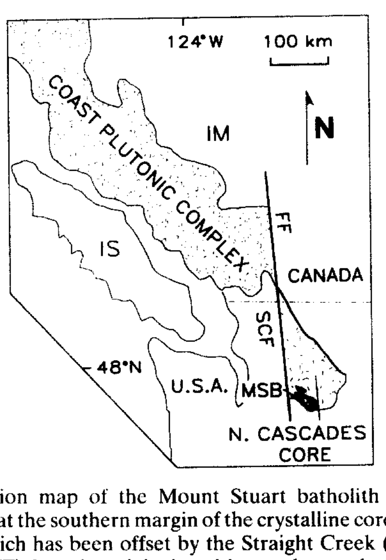

Fig. 1. Location map of the Mount Stuart batholith (MSB). The batholith lies at the southern margin of the crystalline core of the North Cascades, which has been offset by the Straight Creek (SCF)–Fraser River fault (FF) from its original position at the southeast end of the Coast Plutonic Complex. IM = Intermontane superterrane and IS = Insular superterrane.

The *P–T* conditions of the wall rocks at the time of emplacement are less certain. The Chiwaukum Schist records both low *P/T* metamorphism, probably related to emplacement of the batholith, and subsequent relatively static higher-*P* metamorphism that reflects crustal loading (Evans & Berti 1986, Brown & Walker 1993, Miller *et al.* 1993). This complex history hinders interpretation of *P–T* data for the Chiwaukum Schist, which indicate temperatures of 500–700°C for 10 km or more to the northeast of the batholith, and pressures ranging from about 3 to 8 kbar (Plummer 1980, Evans & Berti 1986, Magloughlin 1986, Bendixen *et al.* 1991). A thermal aureole delineated best by synkinematic andalusite extends for 2–3 km from the batholith within the schist (Fig. 2). Regional axial-planar foliation, which is truncated by the batholith, is defined by hornblende in Chiwaukum amphibolites outside of the aureole; thus, the Chiwaukum Schist had reached medium-grade conditions by the time of emplacement. The Ingalls Complex also shows a 1–2 km wide thermal aureole (Fig. 2) (Frost 1975, Miller 1985). Near the Windy Pass thrust the ophiolite was dynamothermally metamorphosed to the amphibolite facies, whereas south of the thermal aureole the complex displays prehnite–pumpellyite and greenschist-facies assemblages that record static, ocean-floor-type metamorphism (Miller 1985). The southern part of the Ingalls Complex thus was considerably cooler than the Chiwaukum Schist at the time of emplacement.

Approximate cooling rates for the batholith can be calculated by comparing the U–Pb zircon ages of the tonalites with K–Ar hornblende and biotite ages. Hornblende ages of 93.2 ± 3.1, 90.0 ± 2.7 and 90.0 ± 2.9 Ma, and biotite ages ranging from 90.0 to 87.7 Ma (Tabor *et al.* 1987) have been reported from three samples within 10 km of the U–Pb localities. Taking standard blocking temperatures for hornblende and biotite (Harrison 1981, Harrison *et al.* 1985) and assuming a solidus of 700°C for the tonalite, cooling rates are on the order of 85–100°C Ma^{-1}, values that are reasonable given the depth of emplacement and the temperature of the wall rocks (cf. Barton *et al.* 1988).

MAGMATIC AND HIGH-TEMPERATURE SOLID-STATE DEFORMATION OF THE BATHOLITH

The Mount Stuart batholith displays a variety of magmatic structures. On a large scale, there are numerous examples of sharp internal contacts between different compositional phases of the batholith. Other igneous features include: (1) compositional banding defined by changes in the percent of igneous minerals or

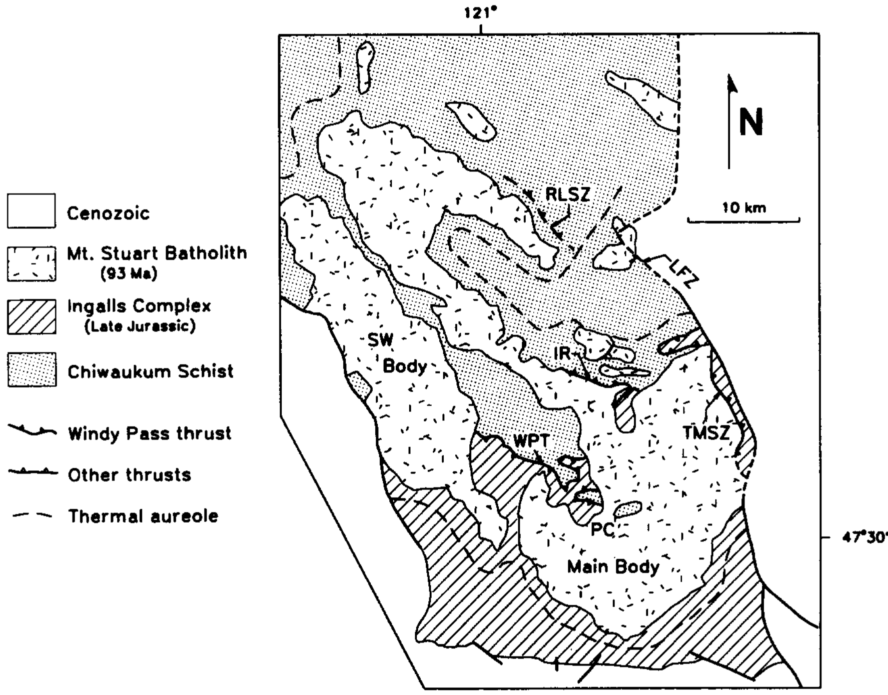

Fig. 2. Map emphasizing the Mount Stuart batholith and areas that display well-developed submagmatic and solid-state deformation. These domains include Icicle Ridge (IR), Pioneer Creek (PC) area near the Windy Pass thrust (WPT), Rock Lake shear zone (RLSZ), and Tumwater Mountain shear zone (TMSZ). LFZ = Eocene Leavenworth fault zone. The thermal aureole is defined by the limit of andalusite in the Chiwaukum Schist and by the serpentine-out isograd in the Ingalls Complex. Modified from Miller & Paterson (1992).

in the textures of these minerals; (2) schlieren layering; (3) individual microgranitoid enclaves or swarms of enclaves, largely of dioritic composition (Anderson & Paterson 1991); (4) dikes; and (5) magmatic foliation and lineation, which everywhere are parallel to or overprint the other igneous features (except for the dikes) and thus formed late in the crystallization history.

Magmatic foliation and lineation are generally well-developed in the margins of the batholith, but the interior displays only weak to moderate magmatic foliation with minor solid-state deformation and recrystallization. Penetrative solid-state deformation overprints well-developed magmatic structures in at least four domains within the batholith (Figs. 2 and 3) (Miller & Paterson 1992). Three of the solid-state domains occur in the northeastern margin of the main body of the batholith, whereas the fourth is near the Windy Pass thrust (Pioneer Creek area). The larger scale patterns of these domains and their tectonic implications are addressed in Miller & Paterson (1992), and are therefore only briefly described here.

The Windy Pass thrust and imbricate thrusts in its upper plate are truncated by the main body of the Mount Stuart batholith (Miller 1985). Tonalites near the thrust, however, show a strong magmatic foliation and a parallel, generally weak to locally moderate solid-state foliation. These relations led Miller & Paterson (1992) to infer that the batholith was intruded during the waning stages of thrusting and that solidification of the tonalite may have arrested thrusting.

Solid-state deformation in the northeastern margin of the main body records both NE–SW contraction and

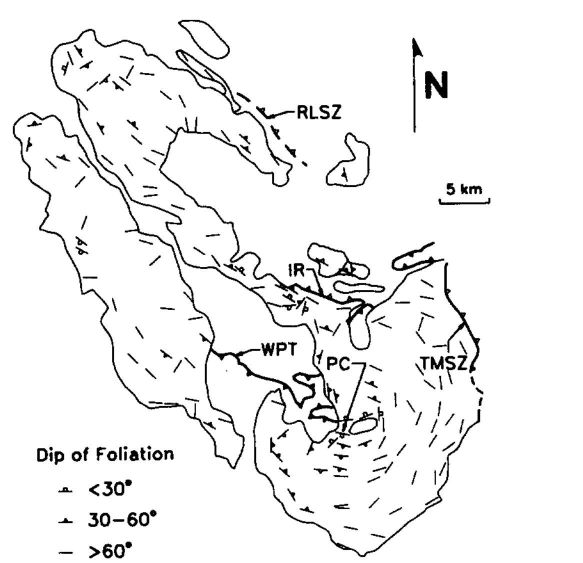

Fig. 3. Map showing foliation patterns in the Mount Stuart batholith. The areas of high strain are labelled as in Fig. 2.

NW–SE stretching (Miller & Paterson 1992). Contraction is best illustrated in the Tumwater Mountain shear zone (Fig. 2), where amphibolite-facies rocks of the Ingalls Complex are thrust to the WSW over the batholith, and near the SW-vergent, reverse-slip Rock Lake shear zone (Fig. 2) (Magloughlin 1990). Along other parts of the northeast margin, magmatic and solid-state foliations and subhorizontal magmatic and solid-state lineations are well developed. These are particularly prominent in the Icicle Ridge area (Fig. 2), which lies near the roof of the batholith. Folds in the adjacent

Chiwaukum Schist record NNE–SSW shortening, and the schists also display a subhorizontal WNW-trending stretching lineation (Miller & Paterson 1992). Several generations of these folds predate the batholith, but folds with similar orientations deform dikes of the batholith (see below), indicating that both folding and subhorizontal WNW-stretching overlapped intrusion. The asymmetry of the various generations of folds and kinematic indicators in local ductile shear zones define SSW-directed thrusting of the schist over the batholith (Miller & Paterson 1992).

These solid-state domains in the pluton and the adjacent wall rocks record all criteria listed above for syntectonic emplacement. In plutonic rocks, solid-state fabrics overprint and are parallel to magmatic fabrics, and they also are parallel to equivalent structures in the wall rocks. Porphyroblasts of andalusite and cordierite, which are restricted to the thermal aureole of the batholith, are syntectonic in the Chiwaukum Schist in the Icicle Ridge area (Plummer 1980, Taylor *et al.* 1991) and in the Ingalls Complex on the southeast side of the batholith. Amphibolite-facies mineral assemblages (hornblende–biotite–plagioclase–quartz) define solid-state fabrics in the batholith (Miller & Paterson 1992). The presence of recrystallized hornblende indicates that most deformation occurred before the tonalites cooled below the blocking temperature of hornblende. Because the K–Ar hornblende ages are within 3.5 Ma or less of the crystallization age of the tonalites, moderate- to high-temperature, solid-state deformation occurred shortly after emplacement, not during a later thermal event. The deformation of the tonalites is essentially syn-emplacement, and the deformation of the batholith was of short duration. In the following, we discuss in more detail the syntectonic structures mentioned above and we more fully document the continuum between magmatic and solid-state deformation shown by the Mount Stuart batholith.

S–C fabrics

S–C structures typify the tonalites in the Tumwater Mountain shear zone, whereas incipient *S–C* fabrics are present locally in the batholith near the Windy Pass thrust. Those in the Tumwater Mountain shear zone indicate the same reverse movement as mylonites in the hanging wall (Miller & Paterson 1992), whereas there are insufficient data near the Windy Pass thrust to interpret kinematics. Microstructures in both areas share many similarities, and we suggest that the incipient fabrics near the Windy Pass thrust preserve the early stages of microstructural development that have been variably overprinted in the Tumwater Mountain shear zone.

The tonalites near the Windy Pass thrust generally record only a strong foliation (*S*) that in a few places is cut by weakly developed *C*-surfaces. Foliation is best defined by large (~3.5 mm long), tabular, euhedral plagioclase crystals (Fig. 4a) that display oscillatory zoning and synneusis. Twin planes and zone boundaries are parallel to grain boundaries. Medium-sized to large isolated grains of hornblende and biotite also lie in the foliation. The strong alignment of these igneous crystals indicates that the foliation is primarily magmatic (e.g. Hutton 1988, Paterson *et al.* 1989).

A weak to moderate solid-state overprint is best displayed by large isolated grains and aggregates of quartz that are elongate parallel to the magmatic foliation. Undulose extinction in quartz is common and subgrains are well developed in the most strongly deformed rocks. Igneous plagioclase is strained, and recrystallized plagioclase is also present.

C-surfaces lie at angles of 25–40° to the *S*-surfaces (Fig. 4a). They are defined by large plagioclase crystals and to a lesser extent by biotite, hornblende and quartz. Plagioclase grains in the foliation and *C*-surfaces are similar in size and show identical twinning and zoning patterns, indicating that the crystals in *C*-orientations are also igneous (Figs. 4a & b). Plagioclase grains in both orientations show deformation twins; some crystals are bent through angles of >20° and locally kinked. Recrystallization of plagioclase to smaller equant grains is modest in both *S* and *C*. This limited solid-state deformation and recrystallization leads us to conclude that the *S–C* fabric formed primarily in the submagmatic state—that is, small amounts of melt allowed rotation and sliding of plagioclase crystals into the *C*-orientation. If grains now in *C* were rotated after the rock was solid, they should display extensive internal deformation and substantial recrystallization to equant crystals due to interference with adjacent grains (e.g. Paterson *et al.* 1989, Vernon *et al.* 1989). Some crystal-plastic flow occurred on *C* after solidification, however, as exemplified by plagioclase grains in *C* that are bent and partially recrystallized by grain-boundary migration. We interpret these relations to indicate that late in the crystallization history of the magma, as igneous minerals began to 'lock-up', shear strain became concentrated in the narrow *C*-surfaces and that this strain partitioning continued during limited plastic flow in the solid state.

In the Tumwater Mountain shear zone, tonalites display *S–C* fabrics (Figs. 4c & d and 5a & b) typical of protomylonitic granitoids sheared at amphibolite-facies conditions (e.g. Simpson 1985). The acute angle between *S* and *C* is generally 20–40°, although there is a pronounced curvature of *S* near *C*-surfaces in some rocks.

Solid-state deformation and recrystallization of all phases is evident in this shear zone. Coarse (~2.5–3.0 mm long), igneous plagioclase is typically bent (Figs. 5a & b) and deformation twins are ubiquitous. This plagioclase is variably recrystallized, in some samples extensively, to small and medium-sized grains (0.15–0.2 mm long) that form polygonal mosaics (Fig. 5b). Some mosaic grains are weakly bent and display deformation twins. The recrystallized plagioclase is about An_{27-28} (determined by standard petrographic techniques and microprobe analyses), similar to the rims of zoned igneous grains. Subgrains are rarely developed, and recrystallization was by grain boundary migration, indicating that the dominant deformation mechanism was recrystallization-accommodated dislocation creep. Quartz displays subgrains and is extensively recrystallized. Although quartz aggregates are elongate in *S* and *C*, they form recrystallized ribbons only in the most strongly deformed rocks. Isolated individual grains of quartz have aspect ratios that reach 3.5:1. Hornblende and biotite in the more strongly deformed rocks only occur as elongate, recrystallized, medium-sized grains in aggregates that are aligned in *S* and *C*. One retort-shaped aggregate of hornblende has tails defined by hornblende and biotite (Fig. 5c). Grains in this aggregate are weakly elongate, show crystallographic preferred orientation as determined with the gypsum plate, and form an oblique foliation inclined to *C*.

Despite this solid-state deformation and recrystallization, evidence of deformation in the magmatic to submagmatic state is preserved. Tabular, euhedral igneous plagioclase crystals provide the best evidence that foliation (*S*) is in part magmatic (Figs. 4c & d and 5a & b). In low strain domains, large aligned hornblende and biotite grains may also be igneous relics. Textures in *C*-surfaces are analogous to those in tonalites near the Windy Pass thrust. In weakly recrystallized rocks the bimodal orientation of large plagioclase grains in *S* and *C* (Fig. 5a) is well displayed. Tabular, euhedral crystals with zone and twin boundaries parallel to grain boundaries are aligned in *C*. Directly adjacent to euhedral plagioclase in *S* are similar-sized crystals in *C* showing identical textures. Grains in both orientations are bent and are partially replaced by a finer-grained mosaic of plagioclase (Fig. 5b). We infer that plagioclase rotated into *C*-orientations while melt was present and that continued shear at subsolidus temperatures was concentrated in *C*-surfaces, resulting in considerable crystal-plastic deformation and local rotation of crystals from *S*- into a *C*-orientation.

Other submagmatic microstructures may be present locally in the Tumwater Mountain shear zone. Apparent tiling (Den Tex 1969, Blumenfeld & Bouchez 1988) of large grains of igneous plagioclase yields the same sense-of-shear as recorded by the *S–C* fabric. Tiling is difficult to prove unequivocally, however, because solid-state antithetic shear along grain boundaries could form an analogous structure. Submagmatic flow is also inferred from large elongate quartz grains aligned in *C*, which show weak subgrain development and little internal strain. Quartz may have crystallized after the critical melt percentage (Arzi 1978, Van der Molen & Paterson 1979) had been reached and other phases had begun to deform in the solid state. Quartz- and feldspar-filled microfractures in plagioclase, which Bouchez *et al.* (1992) consider to be diagnostic of submagmatic flow, have not been observed in the Mount Stuart batholith.

We reiterate that we interpret the microstructures in the Tumwater Mountain shear zone to record a transition from magmatic through submagmatic to solid-state deformation during syn-emplacement reverse slip. We also noted that to document this transition it is important to show that solid-state deformation occurred at high temperatures. The physical conditions under which reverse slip occurred can only be semi-quantitatively estimated, but several observations suggest that the solid-state fabrics formed largely between about 700°C (tonalite solidus) and a minimum of ~550°C.

(1) The recrystallized assemblage (hornblende–plagioclase–biotite–quartz) indicates amphibolite-facies conditions, and there is little or no retrogression of these phases.

(2) Hornblende generally deforms by cataclasis at low to moderate temperatures (e.g. Allison & LaTour 1977, Hacker & Christie 1990) and the absence of microfractures, combined with extensive recrystallization, argues against cataclasis. The high-temperature deformation mechanism of dislocation creep is inferred from features like the retort-shaped aggregate in Fig. 5(c), where weakly to moderately elongate hornblende shows both shape and crystallographic preferred orientations.

(3) Compositions of recrystallized plagioclase are similar to those of the rims of igneous grains and are compatible with only a modest, at most, decrease in temperature from the solidus.

(4) The inferred deformation mechanism for plagioclase of recrystallization accommodated dislocation creep (cf. Tullis & Yund 1985) indicates at least moderately high temperatures, although values are not tightly constrained. The transition from cataclastic flow to recrystallization-accommodated dislocation creep in plagioclase is generally complete by middle to upper amphibolite facies according to Tullis & Yund (1987). The latter mechanism may initiate at temperatures as low as the upper greenschist facies (e.g. Simpson 1985), although others (Olsen & Kohlstedt 1985, Pryer 1993) state that this mechanism indicates temperatures >550°C. The transition from recrystallization by grain boundary migration to climb-accommodated dislocation creep is not well understood (Tullis & Yund 1991). If solid-state deformation in the Mount Stuart batholith initiated at the tonalite solidus, then the absence of climb-accommodated dislocation creep suggests that temperatures were not sufficiently high for this mechanism to be activated, probably because of high strain rates, which we argue below were a likely characteristic of the deformation of the Mount Stuart batholith.

Folding and boudinage

Folds and boudins are best developed along the northeastern margin of the batholith in the Icicle Ridge area, a domain that records strong subhorizontal WNW–ESE stretching in addition to SSW–NNE shortening. Two groups of folds are recognized in this area: folds of tonalites in the margin; and folds of dikes and sills in the batholith and in the wall rocks of Chiwaukum Schist. Boudinaged dikes and sills are most abundant in the wall rocks.

Folds in the margin of the batholith are defined best by magmatic foliation and lineation in the tonalites. They also locally deform microgranitoid enclaves and pegmatites. These folds are typically 10–50 cm in wavelength, range from open to tight with interlimb angles about 30–45°, and display both rounded and angular hinges (Fig. 6a). Axial surfaces are generally steep and subparallel to the dominant axial-planar foliation in nearby Chiwaukum Schist. Axial-planar foliation is well developed along limbs of some tight folds and, in some areas, the axial-planar fabric grades into narrow (up to 10 cm wide) ductile shear zones, indicating shear parallel to the axial planes. These shear zones locally truncate folds and in a few localities numerous small shear zones are associated with swirled folds. Hinge lines are subparallel to mineral lineation (where not folded) in the tonalites and to both stretching lineation and hinge lines in the Chiwaukum Schist.

The folded foliation and lineation record both magmatic and parallel solid-state deformation. There is excellent alignment of tabular, euhedral plagioclase (Fig 5d). These grains are typically bent, but less so than in the Tumwater Mountain shear zone, and there is moderate recrystallization to a fine-grained mosaic. Aggregates of medium-grained biotite and quartz also help define the fabric; quartz forms coarse ribbons in places and displays subgrains and recrystallized grains. In contrast, single grains of hornblende show only weak preferred orientation. Minerals defining the axial-planar foliation display microstructures similar to those of the folded fabric.

We infer that folding occurred under magmatic, submagmatic and high-temperature solid-state conditions. The strongest evidence for this interpretation includes: the swirled appearance of some folds and the overall high ductility of the tonalites; the orientation of hinge lines parallel to magmatic and solid-state lineation in the batholith and to the stretching lineation and hinge lines in the Chiwaukum Schist; and the similarity of the axial-planar fabric to the folded fabric, both of which are marked by magmatic fabrics and amphibolite-facies assemblages.

Besides folds of magmatic foliation within the Mount Stuart batholith, there are many examples of folded and boudinaged dikes of the batholith within the Chiwaukum Schist. These dikes range in composition from tonalite and diorite identical to the main phase of the batholith to more felsic rocks representing late melts. Dike thicknesses rarely exceed two meters; orientations are variable. The dike walls cut across magmatic foliation in the batholith and across the dominant schistosity in the wall rocks. The dikes in both settings in turn are gently to tightly folded. The axial planes of these folds are steep, and fold hinge lines plunge gently to moderately and are parallel to similar elements of folds of foliation in the Chiwaukum Schist (Fig. 6b).

Both magmatic and solid-state foliation are present in the dikes. Weak to moderately intense magmatic foliation can be: (1) parallel to dike walls; (2) parallel to magmatic foliation in the main phase of the batholith, but less intensely developed; (3) folded but with only minor evidence of solid-state deformation; and (4) parallel to the axial planes of the folds, again with little evidence of solid-state deformation. Where present, solid-state foliation is best developed in fold hinges and is parallel to regional foliation.

Some dikes, particularly those with strikes parallel or at a small angle to the trends of regional stretching lineations, show pinch and swell or boudinage (Fig. 6c). Some dikes have relatively rectangular boudins separated by normal faults, whereas others show thinning and thickening indicative of magmatic (little to no solid-state deformation) or ductile (solid-state deformation) flow. Granodiorite and tonalite fill some boudin necks; other necks are dominated by quartz–feldspar veins (Fig. 6c), interpreted to be among the latest melts of the batholith. Dike extension thus occurred at various strain rates and/or while the dikes were in variable rheological states, and while melt was present.

These observations indicate that: (1) both main phase and late phase dikes of the batholith were deformed during emplacement and crystallization; (2) these dikes record deformation over a wide variety of rheological states ranging from magmatic flow to moderate temperature, solid-state deformation; and (3) rates of deformation of the dikes and enclosing rock must have been relatively rapid. For example, the folded dikes with magmatic foliation parallel to the fold axial planes must have been emplaced and folded before the dike could crystallize (i.e. 10^2–10^4 years).

Ductile shear zones

Small ductile shear zones occur near the Windy Pass thrust and in the northeastern margin of the batholith on Icicle Ridge. They are 3–10 cm in thickness, rarely can be traced for as much as 10 m, and have diffuse boundaries. The shear zones are variably oriented and cut magmatic foliation at moderately high angles. Pronounced curvature of foliation into shear zones occurs at some localities, in other places the foliation is swirled erratically, and shear zones may also occur along the limbs of folds (see above). Microgranitoid enclaves are locally offset 10 cm or more across shear zones, but at least one shear zone wraps around an enclave, indicating a significant rheological contrast during shear.

Some ductile shear zones initiated while melt was present (cf. Nicolas 1992), whereas others formed after complete crystallization of the tonalite. Shear zones with swirled foliation record minor solid-state deformation in the form of undulose quartz. Such weak solid-state strain is not compatible with the intensity of deformation in these shear zones, suggesting most slip occurred with melt present. In these zones, the preferred orientation of euhedral igneous plagioclase crystals that are surrounded by weakly to undeformed minerals further supports a magmatic origin. The rheological contrast between enclave and host in the shear zone described above provides additional evidence for magmatic or submagmatic shear.

Slip after tonalite cooled below its solidus is clear where the foliation in shear zones has a solid-state overprint, particularly where the degree of bending and

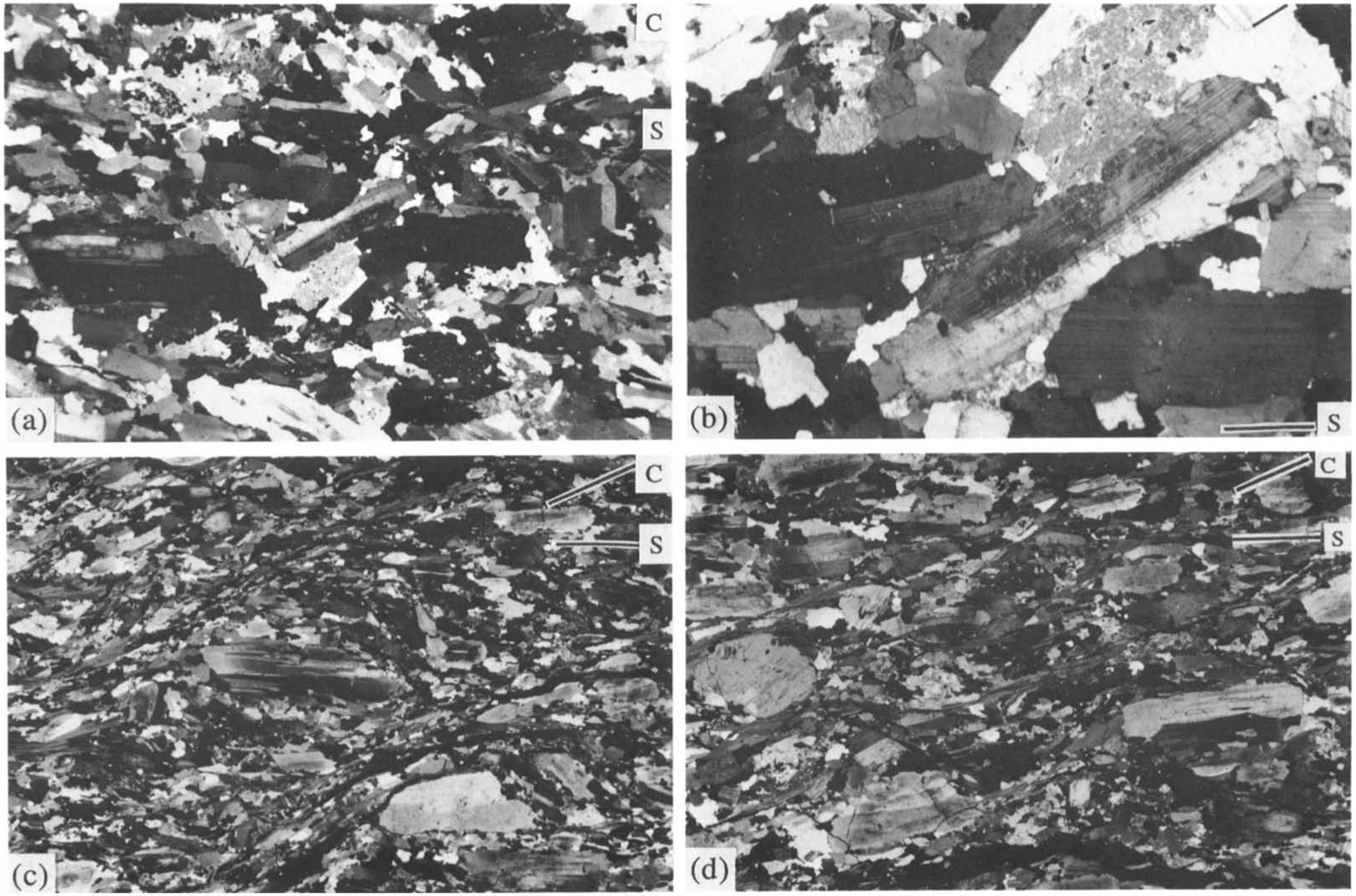

Fig. 4. Microstructures in tonalites from near the Windy Pass thrust and Tumwater Mountain shear zone. (a) Tonalite from near the Windy Pass thrust displaying a well-developed magmatic foliation (trending E–W) defined by large, tabular plagioclase crystals. An incipient submagmatic *C*-surface defined by tabular plagioclase is best seen in the center and lower left part of the figure. Note the relatively weak solid-state deformation. Length of figure is 22 mm. (b) Detail of bimodal fabric defined by igneous plagioclase crystals in tonalite near the Windy Pass thrust. Length of figure is 6.5 mm. (c) Extensively recrystallized *S–C* mylonite from the Tumwater Mountain shear zone. Length of figure is 53 mm. (d) *S–C* mylonite from the Tumwater Mountain shear zone. Biotite best defines *C*-surfaces. Length of figure is 57 mm.

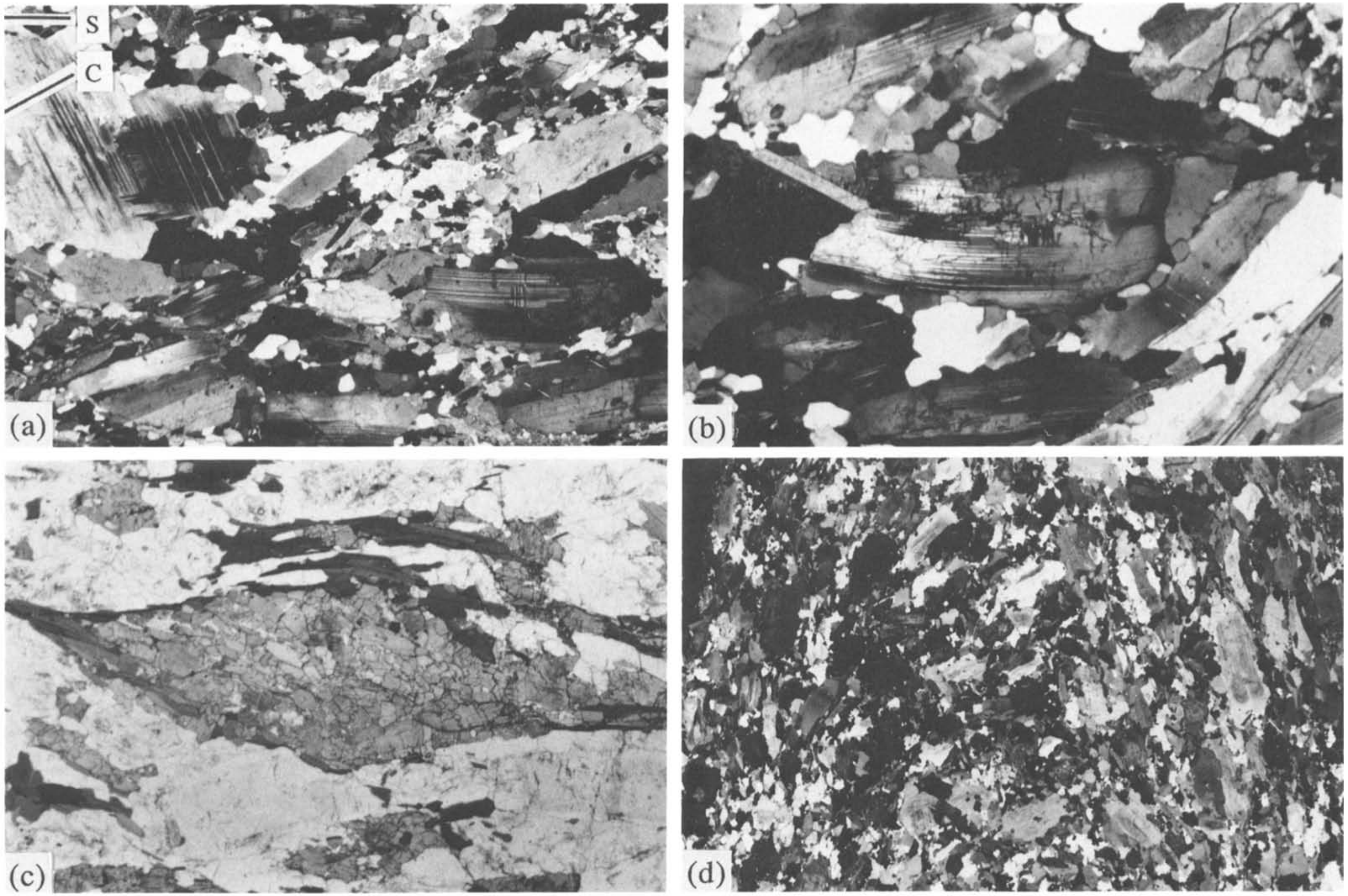

Fig. 5. Microstructures in tonalites from the Tumwater Mountain shear zone and Icicle Ridge area. (a) *S–C* mylonite from the Tumwater Mountain shear zone in which relatively large, tabular, bent plagioclase crystals lie both in *S* and *C*. Note the extensive recrystallization of plagioclase. Length of figure is 6.5 mm. (b) Detail from Tumwater Mountain shear zone showing bent igneous plagioclase grains in both *S*- and *C*-surfaces, and much smaller plagioclase recrystallized by grain boundary migration. Length of figure is 3.3 mm. (c) Recrystallized aggregate of hornblende in mylonitic tonalite from the Tumwater Mountain shear zone. Tails to this aggregate consist of hornblende and biotite (darker mineral). Note that hornblende grains in the aggregate are elongate oblique to the dominant E–W trending foliation. Overall, this aggregate resembles mica 'fish' and gives the same sense-of-shear as determined from the plagioclase-defined *S–C* fabric. Length of figure is 3.3 mm. (d) Hinge zone of fold within tonalite from the northeast margin of the batholith. The fold is best shown by magmatic foliation that is defined by large igneous plagioclase. Length of figure is 30 mm.

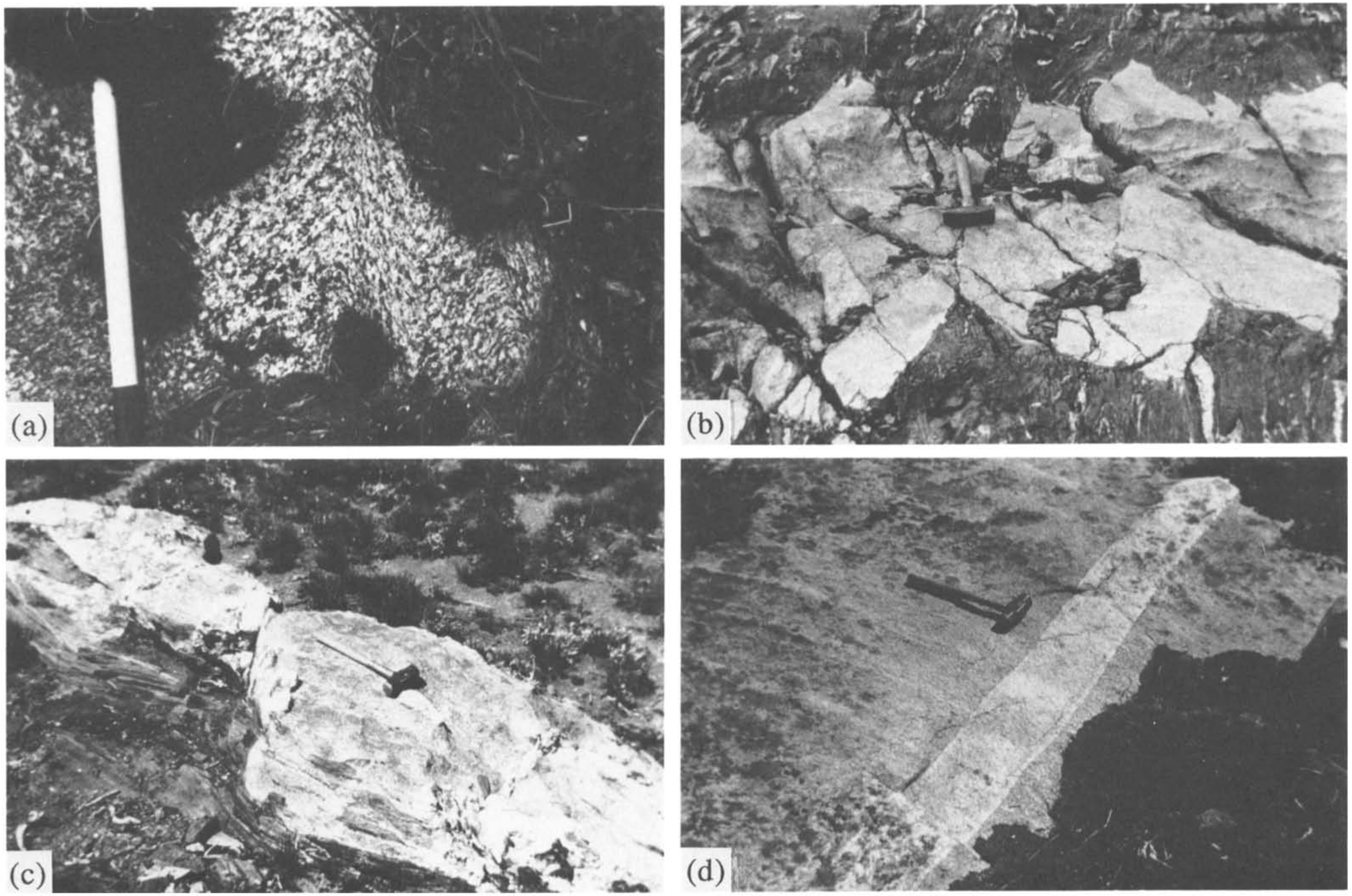

Fig. 6. Mesoscopic structures in the Mount Stuart batholith. (a) Tightly folded magmatic foliation in tonalite from the northeast margin of the Mount Stuart batholith. The hinge line is parallel to magmatic lineation in the tonalite. Pen is 11 cm in length. (b) Folded Chiwaukum Schist and a deformed dike of Mount Stuart tonalite. Mullions in dikes are parallel to the hinge lines. Hammer for scale. (c) Boudinaged sill of Mount Stuart tonalite in the Chiwaukum Schist. Boudin necks are filled by quartz–feldspar veins that probably formed during crystallization from late melts. Hammer for scale. (d) Late felsic dike in the margin of the batholith. Host tonalite has strong magmatic foliation and lineation that have moderate solid-state overprint with similar orientations. Dike is perpendicular to the magmatic and solid-state fabrics of the tonalite. Hammer for scale.

recrystallization of plagioclase increases within a few centimeters of shear zones. The recrystallized assemblage in these shear zones, hornblende–plagioclase–quartz–biotite, is typical of the solid-state deformation of the batholith. An undeformed granitoid veinlet intrudes a shear zone that shows solid-state deformation, implying that deformation occurred shortly after crystallization of the tonalite host but while residual melt was still present.

Mineralized and dike-filled joints

Chloritized and iron-stained joints are intruded by undeformed pegmatite dikes on Icicle Ridge. The joints and dikes are consistently oriented sub-perpendicular to the strong magmatic and solid-state foliation and lineation in the host tonalite (Fig. 6d). The consistency between the extension direction recorded by the joints and dikes and that of the mineral lineation in the tonalite indicates that the joints formed in the early stages of cooling while at least some melt was present to form pegmatite. Furthermore, these relationships document a continuum in dike emplacement and deformation in the Icicle Ridge area from the folded and boudinaged dikes to these late dikes that fill joints.

Low-temperature solid-state deformation

We have emphasized submagmatic and high-temperature solid-state fabrics, but the Mount Stuart batholith also shows less penetrative low- to moderate-temperature (< 500°C) solid-state deformation. The most common of these structures are slickensided surfaces coated by greenschist-facies minerals (actinolite, chlorite). Local upper greenschist-facies ductile shear zones, ranging from 0.5 to 3 m in thickness are concentrated in the mafic phase and the northeastern margin of the batholith. No large brittle structures have been recognized in the batholith.

DISCUSSION

The structural relationships described above show that the northeastern margin of the Mount Stuart batholith was deformed during the transition from magmatic to submagmatic to high-temperature solid-state conditions. Deformation during this continuum was synchronous with 'regional' deformation in the wall rocks of Chiwaukum Schist. The presence of melt during regional deformation thus indicates that the batholith is syntectonic.

A record of a continuous, geologically short-lived transition from submagmatic to high-temperature solid-state deformation is the strongest criterion for syntectonic emplacement, but this transition is not typically reported despite the common interpretation that most plutons are syntectonic. Even in the case of the Mount Stuart batholith, evidence for submagmatic and high-temperature solid-state deformation, and syntectonic deformation in general, is present mainly along the northeast margin of the batholith and in the aureole of Chiwaukum Schist. Most of the batholith displays only minor deformation and recrystallization.

The apparent paucity of plutons recording submagmatic deformation may be in part an artifact of the transitory nature of the submagmatic state (Paterson *et al.* 1989, Paterson & Tobisch 1992, Bouchez *et al.* 1992). Partial melting experiments (Arzi 1978, Van der Molen & Paterson 1979), direct measurements of lavas (McBirney & Murase 1984), and other observations (e.g. Marsh 1981) indicate that material properties of magma change dramatically in the interval between about 50 and 20% melt. During this interval, magma changes from viscous (magmatic) to rigid–plastic (solid state) behavior. Submagmatic behavior is probably restricted to a temperature interval of a few hundred degrees or less (e.g. Cruden 1990). For example, Bouchez *et al.* (1992) show that in the Mont-Louis-Andorra pluton the melt fraction decreased from 30 to 0% over a compositionally dependent interval of 4–63°C. The change from magmatic to solid-state behavior thus probably takes a relatively small percentage of the overall length of time needed to cool a pluton. More specifically, the major change in viscosity occurs over short time periods, usually well below 1 Ma (Paterson & Tobisch 1992), except for very slowly cooling plutons.

It follows from the generally narrow temperature interval for the submagmatic state that syntectonic deformation is most likely to be recorded by slowly cooling plutons and/or by plutons deformed at high strain rates. Paterson & Tobisch (1992) contended that, at mid- and shallow crustal levels, typical strain rates may be too slow to leave an imprint on a crystallizing pluton and only in ductile fault zones are strain rates likely to be rapid enough to form foliations in short timespans. Our observations of the Mount Stuart batholith are compatible with this interpretation. Submagmatic and high-temperature solid-state deformation are best preserved in shear zones along the northeast margin, and dikes within the Chiwaukum Schist adjacent to this margin were deformed at high strain rates (see above). In contrast, deformation in the magmatic state characterizes unsheared segments of the batholith contact, which lack unambiguous evidence for syntectonic emplacement.

Geochronological data indicate relatively normal cooling rates for the Mount Stuart batholith (see above) given its size and the *P–T* conditions of its wall rocks during emplacement. Unusually prolonged cooling through the submagmatic interval is therefore unlikely to have been the dominant factor in the preservation of the transitional structures, although the thermal state of the wall rocks may have been a factor in restricting well-developed submagmatic and solid-state deformation to the northeast margin. The wall rocks of Chiwaukum Schist at this margin record 'regional' metamorphic temperatures in excess of 500°C (e.g. Evans & Berti 1986, Magloughlin 1986) that may have been broadly contemporaneous with pluton emplacement. In contrast, intrusion into the relatively cool wall rocks of the Ingalls Complex led to faster cooling rates in the southern margin of the batholith, thus contributing to the only weak solid-state deformation preserved there.

Two other factors may have facilitated the formation and preservation of submagmatic and other syntectonic structures in the Mount Stuart batholith. Bouchez *et al.* (1992) noted that smaller temperature intervals for the transition from magmatic to solid-state behavior occur in rocks closer in composition to the minima in granite systems and that optimum conditions for preserving submagmatic structures occur in more mafic melts, such as the tonalites of the Mount Stuart batholith. The preservation of syntectonic structures is also enhanced when the deviatoric stresses responsible for submagmatic and high-temperature, solid-state deformation abate before significant sub-solidus deformation obliterates these earlier structures (Bouchez *et al.* 1992). This situation possibly applies to the Mount Stuart batholith where most of the ductile deformation was completed before the pluton cooled below 500°C. However, subsequent, mainly non-penetrative brittle deformation indicates that deviatoric stresses continued to act on the batholith after it had cooled significantly.

The cessation of most ductile deformation of the Mount Stuart batholith before it had cooled substantially below its solidus may account for the differences between the structural style of the batholith and that predicted for deformed cooling syntectonic plutons in general. Gapais (1989) suggested that syntectonic plutons deformed while cooling from high to moderate temperatures may show pervasive *S–C* fabrics that in some cases extend up to the massif scale. During further cooling, strain should become more localized within discrete shear zones. In contrast, *S–C* fabrics are restricted to the margin of the Mount Stuart batholith and lower-temperature, narrow ductile shear zones are uncommon. The large size of the batholith, in combination with other factors discussed above (rates, composition, etc.), may have been a factor in the localization of the submagmatic to high-temperature *S–C* fabrics.

Our analysis of the Mount Stuart batholith and the properties of syntectonic plutons indicates that one setting likely to preserve syntectonic features is the margins of plutons emplaced along fault zones and cooled at moderate rates. Cooling rates and the physical properties of magma are influenced by magma composition, magma and wall rock temperatures, fluids, etc. The optimum cooling rates for preserving syntectonic features apparently occur most commonly in the mid crust. At shallower levels, rapid rates of solidification may not permit the preservation of evidence for synchronous regional deformation and migration of melt (Paterson & Tobisch 1992), and deformation may be dominated by brittle processes. The controls on preservation of syntectonic features are probably more complex at deeper levels. Syntectonic features there may form at lower strain rates than generally required at higher levels, and thus may be more pervasively developed in deeper plutons. In many deep plutons, however, cooling rates may be so slow that syntectonic features are severely overprinted by solid-state deformation and extensive recrystallization. Thus, at deeper levels the preservation of syntectonic features probably depends on the complex interplay between exhumation rates, cooling rates and the duration of deformation. Rapid uplift and/or short interval of deformation presumably would facilitate preservation.

CONCLUSIONS

The Mount Stuart batholith displays a variety of well-developed submagmatic structures that are not commonly described in other syntectonic plutons. Our considerations of the Mount Stuart and other syntectonic plutons suggest the following.

(1) The duration and rates of pluton emplacement and crystallization must be broadly comparable to those of deformation in wall rocks in order to develop and preserve syntectonic structures.

(2) The typical preservation of magmatic structures and the apparent paucity of plutons with well-developed submagmatic structures implies that plutons generally crystallize at much faster rates than they deform. Such relationships may indicate that many plutons are emplaced rapidly as crystal-poor melts while their wall rocks deform rapidly in order to make space for the intrusion; ensuing crystallization is largely static in this interpretation. In the case of relatively crystal-rich syntectonic magmas, the magma-wall rock system is probably dominated by thermal and buoyancy forces, rather than by the regional deviatoric stresses.

(3) Submagmatic structures are best developed in pluton margins. This observation may indicate that the viscous to plastic transition migrates rapidly inward and that the solid rim protects the interior of the pluton, partitioning later slip to the wall rocks. Alternatively, if deformation is waning, the rim may record submagmatic deformation, whereas the interior of a slowly cooling pluton will remain magmatic and have no memory of this deformation.

(4) The preservation of syntectonic features in deep (~30–70 km) crustal plutons probably requires special circumstances, including rapid exhumation and the absence of significant post-emplacement regional deformation. In general, the importance of submagmatic structures in such plutons is not well known.

The questions raised by this discussion emphasize the need for additional detailed studies of strains and strain rates in plutons and their wall rocks. More effort should be focused on aureoles, as most regional analyses of strain rates tend to ignore these rocks because of complications induced by their proximity to plutons. Greater attention should also be given to the development and preservation of syntectonic structures in deep-level plutons.

Acknowledgements—We thank J. L. Anderson for permitting us to refer to his unpublished petrological data. P. Karabinos, M. L.

Williams and S. F. Wojtal gave helpful reviews. D. L. Whitney provided microprobe analyses of plagioclase. The initial stages of manuscript preparation were carried out while the senior author was on leave at the University of Durham and he thanks D. H. W. Hutton for stimulating discussions. This work was supported by National Science Foundation Grants EAR-8917343 (R. B. Miller) and EAR-8916325 (S. R. Paterson).

REFERENCES

Allison, I. & LaTour, T. E. 1977. Brittle deformation of hornblende in a mylonite: direct geometrical analogue of ductile deformation by translation gliding. *Can. J. Earth Sci.* **14**, 1953–1958.

Anderson, J. L. 1992. Compositional variation within the high-Mg, tonalitic Mt. Stuart batholith, North Cascades, Washington. *Geol. Soc. Am. Abs. w. Prog.* **24**, 3.

Anderson, J. L. & Paterson, S. R. 1991. Emplacement of the Cretaceous Mt. Stuart batholith, central Cascades, Washington. *Geol. Soc. Am. Abs. w. Prog.* **23**, A387.

Arzi, A. A. 1978. Critical phenomena in the rheology of partially melted rocks. *Tectonophysics* **44**, 173–184.

Barton, M. D., Battles, D. A., Debout, G. E., Capo, R. C., Christensen, J. N., Davis, S. R., Hanson, R. B., Michelson, C. J. & Trim, H. E. 1988. Mesozoic contact metamorphism in the western United States. In: *Metamorphism and Crustal Evolution of the Western United States* (edited by Ernst, W. G.). Prentice-Hall, Englewood Cliffs, New Jersey, 110–178.

Bendixen, J. E., Morrison, J. & Paterson, S. R. 1991. Thermobarometry of the pelitic Chiwaukum Schist, northern Cascades, Washington. *Geol. Soc. Am. Abs. w. Prog.* **23**, A445.

Blumenfeld, P. & Bouchez, J. -L. 1988. Shear criteria in granite and migmatite deformed in the magmatic and solid states. *J. Struct. Geol.* **10**, 361–372.

Bouchez, J.-L., Delas, C., Gleizes, A. N. & Cuney, M. 1992. Submagmatic microfractures in granites. *Geology* **20**, 35–38.

Brown, E. H. & Walker, N. W. 1993. A magma loading model for Barrovian metamorphism in the southeast Coast Plutonic Complex, British Columbia and Washington. *Bull. geol. Soc. Am.* **105**, 479–500.

Cruden, A. 1990. Flow and fabric development during the diapiric rise of magma. *J. Geol.* **98**, 681–698.

Den Tex, E. 1969. Origin of ultramafic rocks, their tectonic setting and history: a contribution to the discussion of the paper: "The origin of ultramafic and ultrabasic rocks" by P. J. Wyllie. *Tectonophysics* **7**, 457–488.

Erikson, E. H. 1977. Petrology and petrogenesis of the Mt. Stuart batholith—Plutonic equivalent of the high-alumina basalt association? *Contr. Miner. Petrol.* **60**, 183–207.

Evans, B. W. & Berti, J. W. 1986. A revised metamorphic history for the Chiwaukum Schist, North Cascades, Washington. *Geology* **14**, 695–698.

Frost, B. R. 1975. Contact metamorphism of serpentinite, chloritic blackwall and rodingite at Paddy-Go-Easy Pass, central Cascades, Washington. *J. Petrol.* **16**, 272–313.

Gapais, D. 1989. Shear structures within deformed granites: mechanical and thermal indicators. *Geology* **17**, 1144–1147.

Gapais, D. & Barbarin, B. 1986. Quartz fabric transition in a cooling syntectonic granite (Hermitage Massif, France). *Tectonophysics* **125**, 357–370.

Hacker, B. R. & Christie, J. M. 1990. Brittle/ductile and plastic/cataclastic transitions in experimentally deformed and metamorphosed amphibolite. In: *The Brittle–Ductile Transition in Rocks* (edited by Duba, A. G., Durham, W. B., Handin, J. W. & Wang, H. F.). *Am. Geophys. Un. Geophys. Monogr.* **56**, 127–147.

Harrison, T. M. 1981. Diffusion of ^{40}Ar in hornblende. *Contr. Miner. Petrol.* **78**, 324–331.

Harrison, T. M., Duncan, I. & McDougall, I. 1985. Diffusion of ^{40}Ar in biotite: temperature, pressure and composition effects. *Geochim. cosmochim. Acta* **46**, 1811–1820.

Hollister, L. S. & Crawford, M. L. 1986. Melt-enhanced deformation: A major tectonic process. *Geology* **14**, 558–561.

Hutton, D. H. W. 1988. Granite emplacement mechanisms and tectonic controls: inferences from deformation studies. *Trans. R. Soc. Edinb. Earth Sci.* **79**, 245–255.

Karlstrom, K. E. 1989. Towards a syntectonic paradigm for granites. *Eos* **70**, 762–770.

Karlstrom, K. E., Miller, C. F., Kingsbury, J. A. & Wooden, J. L. 1993. Pluton emplacement along an active ductile thrust zone, Piute Mountains, southeastern California: Interaction between deformational and solidification processes. *Bull. geol. Soc. Am.* **105**, 213–230.

Magloughlin, J. F. 1986. Metamorphic petrology, structural history, geochronology, tectonics and geothermometry/geobarometry in the Wenatchee Ridge area, North Cascades, Washington. Unpublished Ph. D. dissertation, University of Washington, Seattle, Washington.

Magloughlin, J. F. 1990. The Rock Lake shear zone: A partial solution to the geological split personality of the Nason terrane. *Geol. Soc. Am. Abs. w. Prog.* **22**, 63.

Marsh, B. D. 1981. On the crystallinity, probability of occurrence, and rheology of lava and magma. *Contr. Miner. Petrol.* **78**, 85–98.

McBirney, A. R. & Murase, T. 1984. Rheological properties of magmas. *Annu. Rev. Earth & Planet. Sci.* **12**, 337–357.

Miller, R. B. 1985. The ophiolitic Ingalls Complex, North Cascades, Washington. *Bull. geol. Soc. Am.* **96**, 27–42.

Miller, R. B. 1988. Fluid flow, metasomatism and amphibole deformation in an imbricated ophiolite, North Cascades, Washington. *J. Struct. Geol.* **10**, 283–296.

Miller, R. B., Brown, E. H., McShane, D. P. & Whitney, D. L. 1993. Intra-arc crustal loading and its tectonic implications, North Cascades crystalline core, Washington and British Columbia. *Geology* **21**, 255–258.

Miller, R. B. & Paterson, S. R. 1992. Tectonic implications of syn- and post-emplacement deformation of the Mount Stuart batholith for mid-Cretaceous orogenesis in the North Cascades. *Can. J. Earth Sci.* **29**, 479–485.

Nicolas, A. 1992. Kinematics in magmatic rocks with special reference to gabbros. *J. Petrol.* **33**, 891–915.

Olsen, T. S. & Kohlstedt, D. L. 1985. Natural deformation and recrystallization of some intermediate plagioclase feldspars. *Tectonophysics* **111**, 107–131.

Paterson, S. R. & Tobisch, O. T. 1988. Using pluton ages to date regional deformations: Problems with commonly used criteria. *Geology* **16**, 1108–1111.

Paterson, S. R. & Tobisch, O. T. 1992. Rates of geological processes in magmatic arcs: implications for the timing and nature of pluton emplacement and wall-rock deformation. *J. Struct. Geol.* **14**, 291–300.

Paterson, S. R., Vernon, R. H. & Tobisch, O. T. 1989. A review of criteria for the identification of magmatic and tectonic foliations in granitoids. *J. Struct. Geol.* **11**, 349–363.

Pitcher, W. S. 1979. The nature, ascent and emplacement of granitic magmas. *J. geol. Soc. Lond.* **136**, 627–662.

Plummer, C. C. 1980. Dynamothermal contact metamorphism superposed on regional metamorphism of pelitic rocks of the Chiwaukum Mountains area, Washington Cascades. *Bull. geol. Soc. Am.* **91**, 1627–1688.

Pongsapich, W. 1974. Geology of the eastern part of the Mt. Stuart batholith, central Cascades, Washington. Unpublished Ph. D. dissertation, University of Washington, Seattle, Washington.

Pryer, L. L. 1993. Microstructures in feldspars from a major crustal thrust zone: the Grenville front, Ontario, Canada. *J. Struct. Geol.* **15**, 21–36.

Simpson, C. 1985. Deformation of granitic rocks across the brittle–ductile transition. *J. Struct. Geol.* **7**, 503–511.

Tabor, R. W., Frizzell, V. A., Whetten, J. T., Waitt, R. B., Swanson, D. A., Byerly, G. R., Booth, D. B., Hetherington, M. J. & Zartman, R. E. 1987. Geologic map of the Chelan 30-minute by 60-minute quadrangle, Washington. *U.S. geol. Surv. Map* **I—1661**.

Taylor, N. W., Paterson, S. R. & Miller, R. B. 1991. Structural analysis of the Chiwaukum Schist in the Mount Stuart region, Central Cascades, Washington. *Geol. Soc. Am. Abs. w. Prog.* **23**, 102.

Tullis, J. & Yund, R. A. 1985. Dynamic recrystallization of feldspar: a mechanism for ductile shear zone formation. *Geology* **13**, 238–241.

Tullis, J. & Yund, R. A. 1987. Transition from cataclastic flow to dislocation creep of feldspar: mechanisms and microstructures. *Geology* **15**, 606–609.

Tullis, J. & Yund, R. A. 1991. Diffusion creep in feldspar aggregates: experimental evidence. *J. Struct. Geol.* **13**, 987–1000.

Van der Molen, I. & Paterson, M. S. 1979. Experimental deformation of partially melted granite. *Contr. Miner. Petrol.* **70**, 299–318.

Vernon, R. H., Paterson, S. R. & Geary, E. E. 1989. Evidence for syntectonic intrusion of plutons in the Bear Mountains fault zone, California. *Geology* **17**, 723–726.

Walker, N. L. & Brown, E. H. 1991. Is the Coast Plutonic Complex the result of accretion of the Insular terrane: Evidence from geochronometry in Washington Cascades. *Geology* **19**, 714–717.